Targeting of Osseous Sites with α-Emitting ^{223}Ra: Comparison with the β-Emitter ^{89}Sr in Mice

Gjermund Henriksen, MSc[1,2]; Darrell R. Fisher, PhD[3]; John C. Roeske, PhD[4]; Øyvind S. Bruland, MD, PhD[5]; and Roy H. Larsen, PhD[1,2]

[1]Department of Chemistry, University of Oslo, Oslo, Norway; [2]Anticancer Therapeutic Inventions AS, Oslo, Norway; [3]Pacific Northwest National Laboratory, Richland, Washington; [4]Department of Radiation and Cellular Oncology, University of Chicago, Chicago, Illinois; and [5]Department of Oncology, Norwegian Radium Hospital, Oslo, Norway

The bone-seeking property and the potential exposure of red marrow by the α-particle emitter ^{223}Ra (half-life, 11.43 d) were compared with those of the β-emitter ^{89}Sr (half-life, 50.53 d). **Methods:** The biodistributions of ^{223}Ra and ^{89}Sr were studied in mice. Tissue uptake was determined at 1 h, 6 h, 1 d, 3 d, and 14 d after intravenous administration. Radiation absorbed doses were calculated for soft tissues and for bone. Multicellular-level doses were estimated for bone marrow cavities. **Results:** Both ^{89}Sr and ^{223}Ra selectively concentrated on bone surfaces relative to soft tissues. The measured bone uptake of ^{223}Ra was slightly higher than that of ^{89}Sr. At 24 h, the femur uptake of ^{223}Ra was 40.1% ± 7.7% of the administered activity per gram of tissue. The uptake in spleen and most other soft tissues was higher for ^{223}Ra than for ^{89}Sr. Although predominant clearance of ^{223}Ra was observed from the soft tissues within the first 24 h, the bone uptake of ^{223}Ra, which was not significantly different from maximum after only 1 h, was not significantly reduced during the 14 d. Furthermore, little redistribution of ^{223}Ra daughter products away from bone was found (2% at 6 h and less than 1% at 3 d). Estimates of dose to marrow cavities showed that the ^{223}Ra α-emitter might have a marrow-sparing advantage compared with β-emitters for targeting osteoid surfaces because the short-range α-particles irradiate a significantly lower fraction of the marrow volumes. At the same time, the bone surfaces will receive a therapeutically effective radiation dose. **Conclusion:** The results of this study indicate that ^{223}Ra is a promising candidate for high-linear-energy transfer α-particle irradiation of cancer cells on bone surfaces. ^{223}Ra can, together with its daughter radionuclides, deliver an intense and highly localized radiation dose to the bone surfaces with substantially less irradiation of healthy bone marrow compared with standard bone-seeking β-emitters.

Key Words: α-particle emitter; ^{223}Ra; ^{89}Sr; bone targeting; dosimetry

J Nucl Med 2003; 44:252–259

Received Sep. 28, 2001; revision accepted Mar. 25, 2002.

For correspondence or reprints contact: Roy H. Larsen, PhD, Anticancer Therapeutic Inventions AS, P.O. Box 54, Kjelsaas, N-0411 Oslo, Norway.
E-mail: roy.larsen@ati-as.no

Bone-targeting radiopharmaceuticals, such as the β-emitters ^{32}P orthophosphate (NaH_2PO_4) and ^{89}Sr (as strontium chloride, Metastron; Amersham Health, Princeton, NJ), have been used extensively for relief of bone pain associated with metastatic lesions in the skeleton (*1*,*2*). Because the major dose-limiting factor with this treatment modality is toxicity to the normal bone marrow cells (*3*–*6*), the range of the β-particles from ^{32}P (maximum energy [E_{max}],1.7 MeV; range, ~6 mm) and ^{89}Sr (E_{max}, 1.49 MeV; range, ~5.5 mm) can be a disadvantage. To minimize marrow toxicity, radionuclides that emit particles of shorter range have been studied for bone pain relief. To date, clinical studies on new radionuclides have been limited mainly to the low-energy β-emitters ^{153}Sm (*7*) and ^{186}Re (*8*), and a conversion electron emitter, ^{117m}Sn (*9*).

Preclinical data on animals and radiation dose estimates indicate that α-particle radiation should be excellent for treating metastatic cancers. The short–α-particle ranges in tissue (<100 μm) match well the small physical size of tumor foci and micrometastases (*10*). α-Emitters have been considered for cancer therapy because their high-linear-energy transfer radiation is more effective at cell killing (*11*) than are the low-linear-energy transfer β-particles. When an α-emitter targets bone surfaces, α-particle crossfire into normal, healthy bone marrow from sources located on the bone surface should be substantially less than the crossfire from β-emitters that are currently approved for clinical use.

In a recent study with ^{211}At and ^{131}I linked to bone-seeking bisphosphonates, a high bone surface–to–bone marrow dose ratio was estimated for ^{211}At relative to ^{131}I (*12*). Other than ^{211}At, only a few other α-particle–emitting radioisotopes are considered useful for biomedical applications (*10*). ^{212}Bi has been evaluated as a bone-seeking agent (*13*,*14*). However, the short physical half-life of ^{212}Bi (60 min) and relatively long times required for bismuth phosphonates to localize in bone result in higher normal-tissue exposure during the uptake and elimination phases (*13*,*14*).

This effect is more pronounced with ^{213}Bi (half-life, 46 min). The β-emitter ^{212}Pb (half-life, 10.6 h) parent has been tried as an in vivo generator for ^{212}Bi. However, a substantial redistribution of ^{212}Pb and ^{212}Bi was observed, resulting in high kidney accumulations of ^{212}Bi (*14*). Other α-emitting radionuclides that are potentially useful in biomedical applications are ^{223}Ra (half-life, 11.43 d) (*15*) and ^{224}Ra (half-life, 3.64 d) (*16*).

^{224}Ra was used medically for many years to treat ankylosing spondylitis (*17–19*). The bone-seeking properties of radium in humans are well known (*17,18*). However, the physical half-lives of ^{224}Ra and its decay products are not ideal for targeting skeletal metastases. As demonstrated in animal experiments, a large fraction of the daughter products of ^{224}Ra escape from bone (*20,21*) because of the noble gas daughter radionuclide, ^{220}Rn (half-life, 55.6 s), which diffuses away from the site of ^{224}Ra decay.

^{223}Ra, another relatively short-lived radium isotope considered for cancer treatment, is likely more suitable as a bone-seeking radiopharmaceutical because its half-life (11.43 d) is about 3 times that of ^{224}Ra. This longer half-life allows greater incorporation into bone surfaces before decay of ^{223}Ra occurs. Thus, a smaller fraction of the total radiation dose will be delivered to soft tissues of the body during the uptake and elimination phase. In addition, the radon daughter, ^{219}Rn, has a very short half-life (3.9 s), which means that the radon will not have sufficient opportunity to diffuse or migrate away from the site of ^{223}Ra deposition.

During the decay of ^{223}Ra and daughter radionuclides, 3 of the 4 α-particles are emitted almost instantaneously as ^{223}Ra decays to stable ^{207}Pb (Table 1). The last α-emitter in the ^{223}Ra chain, ^{211}Bi (half-life, 2.15 min) follows the decay of the β-emitter ^{211}Pb (half-life, 36.1 min), and some biologic redistribution of the last 2 daughters may be expected. If ^{211}Pb is trapped in the bone matrix, the α from ^{211}Bi will irradiate the bone surface area.

Experiments with ^{223}Ra and ^{89}Sr (half-life, 50.53 d) were conducted to determine relative uptake in soft tissues and bone. This article describes a dosimetric analysis of ^{223}Ra and ^{89}Sr on bone surfaces of mice and the degree to which surface deposits irradiate healthy red marrow.

MATERIALS AND METHODS

Radionuclides

^{223}Ra was produced from an ^{227}Ac generator system, as described elsewhere (*22*). Briefly, ^{227}Ac and ^{227}Th were immobilized on an actinide-selective resin to allow highly effective retention of actinium and thorium under conditions at which ^{223}Ra elutes. The solution containing purified ^{223}Ra was evaporated to dryness. The ^{223}Ra activity was dissolved in isotonic saline with 5 mmol/L ammonium citrate, pH 7.4. Prior to injection, the solution was filtered through sterile 0.22-μm nylon filters (Nalgene, Rochester, NY).

γ-Radiation emitted by ^{223}Ra and several of its decay products is useful for determining the quality and quantity of radionuclides in biologic samples. ^{223}Ra has a characteristic γ-peak at 154.2 keV (5.59% abundance) (*23*), and ^{211}Bi has a γ-peak at 351.1 keV (12.8%). These photons may be used to determine whether daughter products redistribute in living systems. ^{223}Ra also has a 269.4-keV peak (13.6%), which is difficult to distinguish from the ^{219}Rn peak at 271.23 keV (9.9%).

^{89}Sr-Chloride (Metastron; Amersham Health, Buckinghamshire, U.K.) was diluted to the desired activity concentration with sterile saline solution.

Biodistribution Experiments

All procedures and experiments involving animals in this study were approved by the National Animal Research Authority (Norway) and were performed according to the European Convention for the Protection of Vertebrates Used for Scientific Purposes (*24*).

^{89}Sr-Chloride and ^{223}Ra-chloride were administered to mice by tail vein injection using 100–150 μL of solution. Young male BALB/c mice with body weights of 19–21 g were injected with 9 kBq of ^{223}Ra or 3 kBq of ^{89}Sr. Groups of mice were sacrificed and dissected at 1 h, 6 h, 24 h, 3 d, and 14 d after injection. Activity levels chosen were those that were deemed optimum for biodistribution analysis and counting on the analysis system at these time points. The tissue uptake of ^{223}Ra and decay products was measured with the radionuclides in radioactive equilibrium; tissue samples were stored for at least 5 half-lives of ^{211}Pb before the samples were measured. Two measurement procedures were used: In the first, tissue samples were counted using a NaI(Tl) well-type detector (Harshaw Chemie BV, De Meern, Holland) combined with a scaler timer ST7 digital unit (NE Technology Ltd., Reading, U.K.); in the second, samples were measured by liquid scintillation counting. In this procedure, soft-tissue samples were dissolved by adding 1–3 mL of Soluene 350 (Packard, BioScience BV, Gro-

TABLE 1
α- and β-Radiation Emitted in Decay Chain of ^{223}Ra

Parameter	^{223}Ra	^{219}Rn	^{215}Po	^{211}Pb	^{211}Bi	^{207}Tl
Half-life	11.43 d	3.96 s	1.78 ms	36.1 min	2.17 min	4.77 min
α-Energy (mean) (MeV)	5.64	6.75	7.39		6.55	
β-Energy (maximum) (MeV)				1.37		1.42
Energy fraction*	0.207	0.248	0.271	~0.017	0.24	~0.017

*Relative to total emitted energy for complete decay chain. Energy from emitted radiation associated with decay of ^{223}Ra and daughters is ~27.5 MeV. Fraction of energy borne by particulate radiation emitted as α-particles is ~97%. Fraction of energy emitted as β-particles is ~3%.

ningen, Holland) per 100 mg of tissue. Bone samples were dissolved in $HClO_4$:H_2O_2 1:2 (v/v). All tissue samples were maintained at 50°C until they were completely dissolved. If required, soft-tissue samples were bleached with H_2O_2. Insta-Gel Plus II scintillation cocktail (Packard) was added, and the samples were stored in the dark to avoid interference from room luminescence. The ^{89}Sr content of mouse tissues was also determined by liquid scintillation counting, as described above for ^{223}Ra.

Reference standards of ^{223}Ra (in equilibrium with daughter radionuclides) and ^{89}Sr were used during tissue analyses.

To investigate the redistribution of decay products from ^{223}Ra, samples of blood, liver, and kidney were studied immediately after dissection using a solid-state germanium detector (Canberra, Meriden, CT) combined with an amplifier and bias supply from EG&G Ortec (Oak Ridge, TN).

Retention of Progeny from ^{223}Ra Located in Bone

To examine the differences in radionuclide retention between ^{223}Ra and ^{211}Bi in bone samples, γ-spectroscopy was performed on bone samples and compared with data from a standard solution of ^{223}Ra in equilibrium with its daughters. γ-Spectroscopy with the germanium detector was performed on samples of femur immediately after the mice had been sacrificed and dissected. The distinct γ-peaks at 351.0 keV (^{211}Bi) and 154.2 keV (^{223}Ra) were used for this analysis. For ^{223}Ra, a localization index based on the relative counting rate (CR) of ^{223}Ra and ^{211}Bi in samples versus standard was determined as (CR of ^{211}Bi in sample/CR of ^{211}Bi in standard)/(CR of ^{223}Ra in sample/CR of ^{223}Ra in standard).

For statistical analysis, γ-spectra from 5 samples from the 6-h group and from the 3-d group, respectively, were compared with 5 and 3 samples from the standard solutions, respectively. The Student *t* test was used to determine statistical differences between the groups.

An additional experiment was conducted to investigate the potential release of ^{223}Ra progeny from bone. Femurs from 5 mice sacrificed at 6 h and from 5 mice sacrificed 3 d after injection were examined. The bones were cleaved longitudinally, to expose the red marrow, and thereafter were cut into small pieces of less than 3 mg each. The bone samples were washed with Dulbecco's phosphate-buffered saline (Sigma-Aldrich Co., Ltd., Irvine, U.K.) using centrifugation. The supernatant, including dissolved bone marrow, was removed, mixed with scintillation liquid (Insta-Gel Plus II), and counted on a scintillation counter (Beckman Instruments Inc., Fullerton, CA). Sample counting was repeated after 1 d. The difference in counts after correcting for ^{223}Ra decay between the 2 measurements was used to identify the release of daughter radionuclides from bone matrix.

Dosimetry Calculations

Tissue absorbed doses for ^{223}Ra (and daughters) and ^{89}Sr were determined, and their localized energy distributions were calculated using both multicellular dosimetry and standard dose-averaging methods (*25*,*26*). The trabecular bone was modeled as a solid matrix of bone mineral containing a high density of spheric marrow cavities. The surface-to-volume ratios for bone, as described by the International Commission on Radiological Protection (*27*), were assumed to hold true for the mice in this study. Marrow cavities of 3 different spheric sizes (radii = 50, 150, and 250 μm) were considered, and doses were calculated assuming an activity of 0.67 Bq/mm^2 ^{223}Ra and 20.42 Bq/mm^2 ^{89}Sr on the bone surfaces of these cavities. The activities of ^{89}Sr and ^{223}Ra used in these calculations corresponded to those projected to result in a total absorbed dose of 10 Gy to bone. Instantaneous uptake and infinite biologic retention of the activity at bone surfaces were assumed.

Methods using the standard MIRD formalism were described previously by Fisher and Sgouros (*28*) for assessing the localized dosimetry of ^{223}Ra and daughter products. Briefly, the absorbed dose is the product of all the energies emitted by ^{223}Ra and daughters that are absorbed locally in the target mass, divided by the mass of the target, integrated over time. The principal α-, β-, and γ-ray emissions of ^{223}Ra and daughters were included in this analysis. The absorbed dose (Gy) to a target region (r_k) from a source region (r_h) resulting from an internally administered radionuclide (*29*,*30*) is:

$$\text{Dose} = \tilde{A}_h S_{(r_k \leftarrow r_h)}, \qquad \text{Eq. 1}$$

where $\tilde{A}_h$ is the cumulated activity or total number of transformations (Bq s) that have taken place in the source tissue (r_h), and S (Gy Bq^{-1} s^{-1}) is the mean dose to a target tissue (r_k) per unit cumulated activity in the source tissue. The cumulated activity $\tilde{A}_h$ in a source region (r_h) is the total number of radioactive transformations over time *t* (infinite time), accounting for both radioactive decay and biologic clearance:

$$\tilde{A}_h = \int_0^\infty A_h(t)\, dt. \qquad \text{Eq. 2}$$

The cumulated activity was determined by integrating a time–activity curve obtained from the counting results for each tissue using least squares regression.

The S value is the product of the reciprocal mass m_k (g) of the target organ or tissue and the sum of the products of the dose constant (mean energy emitter per nuclear transition, or Δ_i, in Gy kg Bq^{-1} s^{-1}) and the energy absorbed fraction of the *i*th emission (ϕ_i):

$$S_{(r_k \leftarrow r_h)} = 1/m_k \sum^{i} \Delta_i \phi_i. \qquad \text{Eq. 3}$$

The absorbed fraction (ϕ_i) is the fraction of energy emitted by the *i*th emission from activity in the source region that is absorbed in the target region. These fractions were calculated for the α- and β-energies characteristic of each of the major emissions from ^{223}Ra and daughters, and from ^{89}Sr. The equilibrium dose constant Δ_i is the sum of the products of a unit conversion constant (*k*), the fractional abundance of each emission (n_i), and the energy of the *i*th emission (E_i):

$$\Delta_i = \sum^{i} k n_i E_i. \qquad \text{Eq. 4}$$

The equilibrium dose constant for ^{223}Ra and daughters through complete decay of the ^{223}Ra decay chain is 4.51×10^{-12} Gy kg Bq^{-1} s^{-1} (60.0 g rad μCi^{-1} h^{-1}). A total of 28.2 MeV of energy is liberated by this decay chain, of which 93% is by α-particle emission.

The equilibrium dose constant for ^{89}Sr is 9.32×10^{-14} Gy kg Bq^{-1} s^{-1} (1.24 g rad μCi^{-1} h^{-1}). The mean energy of the β-particle from ^{89}Sr is 0.583 MeV (E_{max} = 1.492 MeV). The absorbed fractions of β-energy in bone and soft tissues were determined using Berger's point kernels for absorbed-dose distributions of β-particles in unit-density medium, scaled by interpolation to

compact bone density ($\rho = 1.85$), and assuming point sources for ^{89}Sr (*31*,*32*).

α-Particle doses with depth in marrow were calculated using the method described by Roeske et al. (*25*). Briefly, the dose $D_{(r)}$ at a particular point is given by:

$$D(r) = \int f(\vec{r} - \vec{r}')A(\vec{r}')d\vec{r}'^2, \qquad \text{Eq. 5}$$

where $f(\vec{r} - \vec{r}')$ is the dose point kernel representing the dose deposited as a function of radial distance from a point source located at $\vec{r}'$. The quantity $A(\vec{r}')$ is the intensity of the source per unit area. The dose point kernel for ^{223}Ra is given by:

$$f(\vec{r} - \vec{r}') = \frac{1}{4\pi|\vec{r} - \vec{r}'|^2} \sum a_i \frac{dE(\vec{r} - \vec{r}')_i}{dx}, \qquad \text{Eq. 6}$$

where a_i is the fractional contribution from the i^{th} α-particle, and *dE/dx* is the linear energy transfer function based on data from the International Commission on Radiation Units and Measurements (*26*). In using this form for the dose point kernel, we assumed that the α-particles travel in straight lines and lose energy through the continuous slowing-down approximation. Thus, negligible scattering and statistical fluctuations in energy deposition along the particle path were assumed valid. In addition, the range of δ-rays and the width of the α-particle track (~100 nm) were ignored since the target that is often considered (i.e., cell nucleus) is much larger than these dimensions (*33*). Equation 5 was evaluated using numeric integration.

RESULTS

Biodistribution of ^{89}Sr and ^{223}Ra

The uptake of ^{223}Ra and ^{89}Sr in selected tissues of mice is shown in Figures 1 and 2, respectively. Additionally, the uptakes of ^{89}Sr, ^{223}Ra, and decay products in samples of brain and heart were measured and found to be insignificant at all time points. The results showed that ^{223}Ra selectively concentrated in bone, compared with the concentration in soft tissues. Although all the soft-tissue values decreased in radionuclide concentration between 1 h and 3 d after injection, the bone activity concentrations had already reached a level close to maximum after 1 h, with no statistically significant change in the levels during the 14 d. After 24 h, the percentage of injected dose per gram of femur tissue was 40.1 ± 7.7. For ^{89}Sr, the corresponding value was 17.7 ± 2.8. At 14 d, the values for ^{223}Ra and ^{89}Sr were 31.1 ± 2.6 and 21.1 ± 2.7, respectively. For ^{223}Ra, the femur-to-blood ratio increased from 118 to 691 within a period of 1 h to 3 d. Kidneys and spleen had the highest retention of ^{223}Ra among the soft tissues. However, the femur-to-kidney ratio also increased with time, from 1.9 to 91 between 1 h and 3 d after injection. The femur-to-spleen ratio was also 1.9 at 1 h but increased to 24 at 3 d after injection. The femur-to-kidney and femur-to-spleen ratios of ^{223}Ra were lower than the ratios for ^{89}Sr.

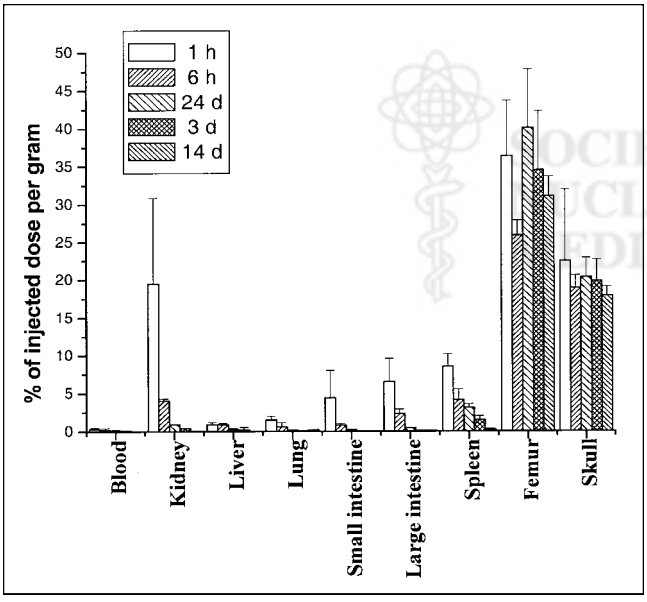

FIGURE 1. Uptake of ^{223}Ra in organs and tissues of mice. Columns represent mean ± SD of percentage injected activity per gram of tissue for groups of 5 mice per time point.

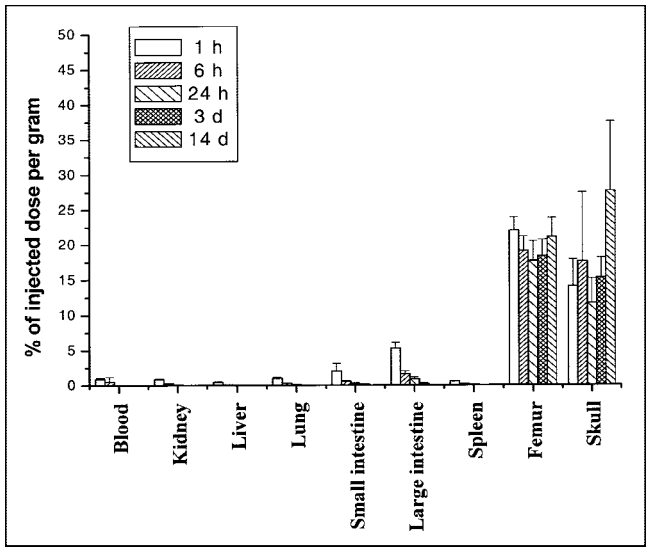

FIGURE 2. Uptake of ^{89}Sr in organs and tissues of mice. Columns represent mean ± SD of percentage injected activity per gram of tissue for groups of 5 mice per time point.

Retention of Progeny from ^{223}Ra Located in Bone

The average ratio of ^{211}Bi to ^{223}Ra in the spleen at 6 h was 0.54, compared with a standard solution. In liver and kidneys, the average ^{211}Bi-to-^{223}Ra ratios were, respectively, 2.56 and 2.07 times those of the standards. These results indicated that some migration of ^{223}Ra daughters occurred in soft tissues. The ^{211}Bi activity in soft tissues was low, compared with that in bone. The presence of ^{211}Bi in soft tissues likely resulted from ^{223}Ra in soft tissues.

In bone, the average localization index for the ^{211}Bi-to-^{223}Ra ratio was 0.85 ($P = 0.059$, $n = 5$) at 6 h and 0.97 ($P = 0.749$, $n = 5$) at 3 d; that is, the differences were not significant.

Mice sacrificed after 6 h showed some release of ^{223}Ra daughter activity from bone. Compared with the total activity in bone, 1.8% dissolved (mean value) in phosphate-buffered saline during washing. When the washing solutions were counted again after 12 h, the activity was, on average, only 0.2% of that in the bone sample. This result indicated that less than 2% of the ^{223}Ra daughter radionuclides migrated away from bone surfaces. Femurs from mice that were sacrificed after 3 d showed no significant ^{223}Ra decay product counts, compared with background levels in the washing solution. This result indicated that migration of ^{223}Ra decay products, if it occurred, was less than our detection limit and also less than about 1% of the total radioactivity in bone.

Dosimetry

As described above, the radionuclide source cumulated activities were calculated by integrating the time–activity curves obtained from the ^{223}Ra and ^{89}Sr biodistribution studies. The animal biodistribution data (Fig. 1) confirmed that the assumption of instantaneous uptake and infinite retention in bone was a valid approximation since both radionuclides reached an activity level equivalent to maximum only 1 h after injection and the radioactivity levels in bone did not change significantly up to 14 d. Table 2 shows our absorbed dose estimates to bone and soft-tissue samples (mGy) per 1 kBq administered per gram of body weight. As can be seen from Table 2, dosimetry indicated a greater radiation absorbed dose to soft tissues per kilobecquerel of activity for ^{223}Ra than for ^{89}Sr because of the lower decay energy of ^{89}Sr than for ^{223}Ra.

The mean of the radiation absorbed doses to femur, skull, and rib (Table 2) was used as an average dose estimate for bone. Based on this value, the activity needed to produce an absorbed dose to bone of 10 Gy was calculated. From the activity value and from the absorbed dose estimates (mGy/kBq per gram of body weight; Table 2), the corresponding absorbed doses to soft tissue were calculated. Table 3 shows the absorbed doses to soft tissues for a total estimated absorbed dose to bone of 10 Gy. This method predicts higher radiation doses to the kidneys, lungs, intestines, and spleen from ^{223}Ra than from ^{89}Sr.

TABLE 2
Radiation Absorbed Dose Estimates

	^{223}Ra		^{89}Sr	
Organ	Absorbed fraction	Dose	Absorbed fraction	Dose
Kidney	1	572.11	0.73	0.74
Liver	1	136.54	0.82	0.41
Lung	1	81.40	0.66	1.52
Small intestine	1	108.00	0.81	1.72
Large intestine	1	264.65	0.75	4.41
Spleen	1	1,151.02	0.6	0.43
Femur	0.95	36,664.85	0.4	974.84
Skull	0.95	21,401.19	0.4	1,230.88
Rib	0.95	16,668.65	0.4	242.63

Doses are expressed as mean absorbed dose in mGy/kBq injected activity per gram of body weight.

TABLE 3
Absorbed Doses Estimated for Soft-Tissue Organs

Organ	^{223}Ra	^{89}Sr
Kidney	0.229	0.009
Liver	0.055	0.005
Lung	0.033	0.018
Small intestine	0.043	0.021
Large intestine	0.106	0.054
Spleen	0.462	0.005

Dose estimates (Gy) for selected soft-tissue organs resulting from activity of ^{223}Ra and ^{89}Sr calculated to give average dose of 10 Gy to bone. This corresponds to injected activities of 0.4 kBq/g and 12.2 kBq/g, respectively. Dose estimate for bone was based on average value from 3 bone specimens presented in Table 2.

Figure 3 shows the results of small-scale, localized dose calculations for ^{223}Ra and ^{89}Sr distributed on the bone surface of marrow cavity spheres having radii of 50, 150, and 250 μm. The activities of ^{89}Sr and ^{223}Ra used in these calculations corresponded to those projected to result in a total absorbed dose of 10 Gy to bone. For ^{223}Ra, the estimated absorbed dose in a 250-μm sphere decreased steeply from approximately 65 Gy at 5 μm from the surface to 0 Gy at about 70 μm, the energy-range cutoff distance. For a 150-μm sphere, the absorbed dose decreased steeply with distance from 75 Gy at 3 μm to 0 Gy at 69 μm. For a 50-μm sphere, the absorbed dose decreased from 97 Gy near the bone surface to about 60 Gy in the least exposed volume.

By comparison, only small changes in absorbed dose from ^{89}Sr, with distance from surface, were observed from the dose calculations. The implications of this dosimetry are important to understanding the potential differences between ^{223}Ra and ^{89}Sr with respect to marrow toxicity. This work shows that the principal advantage of α-particle emitters for targeting osteoid surfaces is that substantial volumes in the trabecular marrow cavities would receive very low radiation doses from ^{223}Ra, compared with ^{89}Sr, per unit bone surface dose and that the sparing of normal red marrow would have important clinical significance for the patient. ^{223}Ra could produce a clinically more effective and substantially greater bone surface dose for therapeutic benefit while minimizing the radiation absorbed dose and associated hematopoietic suppression associated with localized irradiation of red marrow.

DISCUSSION

A desirable approach to treating metastatic cancer in the skeleton with bone-seeking radionuclides would be to use radiopharmaceuticals that deliver a high dose to the bone lesions while sparing bone marrow. Because of their short

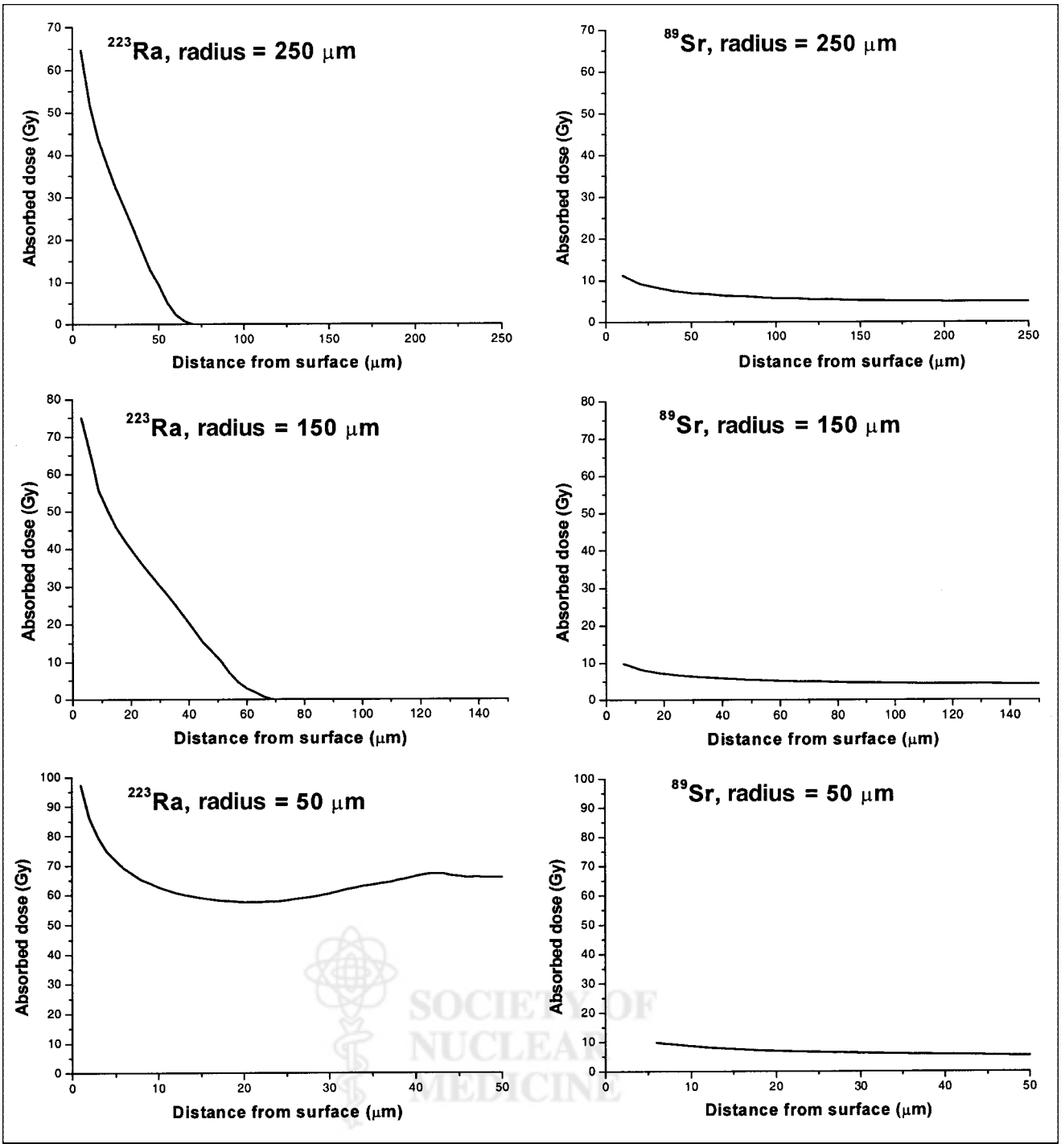

FIGURE 3. Dose estimates for ^{223}Ra and ^{89}Sr distributed on surface of spheres of radii 50, 150, and 250 μm. Activity of 0.67 Bq/mm^2 was assumed for ^{223}Ra, and activity of 20.42 Bq/mm^2 was assumed for ^{89}Sr.

range corresponding to the physical dimensions of single cancer cells and micrometastases, high-linear-energy transfer, dose-rate independence, and effective cell-killing efficiency (*34*), α-emitters have outstanding potential for treating metastatic cancer. Compared with other α-emitting radionuclides for targeted radiation therapy, ^{223}Ra has several favorable properties. ^{223}Ra may be produced relatively inexpensively and in large amounts from ^{227}Ac (half-life, 21.7 y), which can be obtained by neutron irradiation of ^{226}Ra target material. The relatively long physical half-life of ^{223}Ra (11.4 d) is advantageous for generating source material, shipping material, and preparing and administering the radiopharmaceutical yet is short enough to avoid generating long-lived radioactive hospital waste. The use of

^{223}Ra in clinical settings is also favored from a practical standpoint. Compared with therapy with other radionuclides, ^{223}Ra requires less shielding because the fraction of penetrating radiation is low for the ^{223}Ra decay series. Radiation exposure to medical staff would therefore be much less for ^{223}Ra than for several other α-emitting radionuclides.

In skeleton-targeted therapy, the rapid α-particle cascade from ^{223}Ra has potential to deliver high radiation doses to tumors. With regard to concerns on the redistribution of daughter products, any potential application of ^{223}Ra must account for the potential increased radiation exposure to normal organs and tissues. Thus, the biologic distribution of both the parent radionuclide and the decay products must be considered carefully. In the present study, bone samples from mice injected with ^{223}Ra were studied by γ-ray spectroscopy, and the relative bone content of ^{211}Bi versus ^{223}Ra was determined immediately after dissection. The results of this research indicated that only very small amounts of ^{223}Ra daughter radionuclides redistributed from the site of ^{223}Ra decay in bone. Based on the extractable radioactive fraction from finely fragmented bone samples, it was found that the outward translocation of ^{223}Ra daughter products from the bone matrix was low. Short-lived activity was observed in the supernatant from finely fragmented bone samples at 6 h. However, the released activity at 3 d after injection was estimated to be less than 1% of the total bone content of ^{211}Pb and ^{211}Bi. This finding indicated that even for the ^{211}Bi transformation (the fifth transformation in the series from ^{223}Ra), the retention of decay products in bone was similar to that of the parent ^{223}Ra. Additionally, this finding represents an important argument to counter the concerns over redistribution of ^{223}Ra daughter products from the targeted tissue. Prior studies of ^{224}Ra in beagles showed a significant redistribution of ^{212}Pb and ^{212}Bi from ^{224}Ra-deposited bone (*20*). The retention of ^{212}Pb and ^{212}Bi in bone increased with time and reached a plateau at approximately 80% and 70% of their equilibrium values, respectively, at about 2 d after injection (*20*). The present study on ^{223}Ra and the existing data on ^{224}Ra produced the following conclusions about the differences between ^{223}Ra and ^{224}Ra when used as bone-targeting agents: First, ^{223}Ra has a longer physical half-life than ^{224}Ra, which shifts the bone–to–soft-tissue ratios to higher values because a larger fraction of ^{223}Ra is eliminated from soft tissue before decay occurs. Second, the longer half-life of ^{223}Ra than of ^{224}Ra allows greater incorporation into the bone surfaces during bone remodeling. This effect may contribute to better retention of daughter products, which could otherwise redistribute because of diffusion and α-recoil. Third, the radon daughter of ^{223}Ra (^{219}Rn) has a shorter half-life than that of ^{224}Ra (^{220}Rn), resulting in substantially less redistribution of daughter radionuclides from the ^{223}Ra series.

In the current study, bone uptake of ^{223}Ra in mice was found to be high and selective compared with uptake in the soft tissues. In addition, ^{223}Ra was well retained in bone. The biologic elimination of ^{223}Ra from soft tissues was rapid, compared with its half-life. ^{223}Ra was found to have a high bone uptake, confirming work by others that showed radium to be an excellent bone-seeking element. This study used normal mice. Alternatively, tumor-bearing animals could have been used. The current study represents an initial effort to evaluate ^{223}Ra as a potential treatment for bone metastases. Because few data have been published on ^{223}Ra, we chose to use normal immune-competent animals without tumors to study the basic metabolism of the compound, since animals with skeletal metastases could have significantly altered biokinetics due to increased bone metabolism in the tumor area. Also, ^{223}Ra could be particularly effective to sterilize the bone surfaces against microdeposits of cancer cells (e.g., in the preosteoblastic stage of metastasis development). Several studies have focused on the use of agents to prevent development of future skeletal events (*35–37*). It is therefore interesting to evaluate, as a prelude to future experiments in tumor models, whether the normal bone uptake of ^{223}Ra could deliver substantial doses with the potential to sterilize bone-surface–deposited micrometastases (*38*).

Doses were estimated using macroscopic and small-scale dosimetric techniques. The results of dose calculations from the biologic data showed that for a given dose to bone, ^{223}Ra provided a greater dose to some soft tissues (kidneys, spleen) than did ^{89}Sr (Table 2). However, ^{223}Ra also provides a high, intensely localized radiation dose at bone surfaces (Fig. 3), meaning that a relatively low administered activity will produce a therapeutically relevant dose with little consequence to kidneys and spleen. Moreover, the concentration of radiation energy close to bone surfaces results in substantial sparing of healthy red marrow, the critical organ for normal-tissue toxicity in skeleton-targeted radionuclide therapy of osteoid neoplasms. With assumed marrow cavity sizes of 150 and 250 μm in trabecular bone, and assuming 0.67 Bq/mm^2 of ^{223}Ra, an estimated dose to the surface of about 70 Gy is delivered. On the basis of these estimates, healthy red marrow in the adjacent bone cavities will receive total radiation doses that are much lower than those resulting from ^{89}Sr under comparable circumstances, allowing a greater fraction of marrow cells to survive treatment. That relatively large amounts of the ^{223}Ra can be tolerated has been indicated in a pilot study in which mice injected with 1 kBq of ^{223}Ra per gram of body weight were followed for 3 mo without showing signs of life-threatening acute toxicity (*38*). This finding indicates that bone marrow and soft-tissue organs could withstand therapeutically relevant levels of ^{223}Ra.

In the current study, we used a simplistic geometric representation of the bone marrow cavities to compare the relative merits of 2 radionuclides. A more sophisticated analysis would involve performing 3-dimensional dosimetry calculations based on realistic tumor and bone marrow geometries. Such analyses for bone marrow have been performed by Akabani and Zalutsky (*39*) and by Charlton et al.

(*40*). In both cases, histologic samples of bone marrow were obtained from either beagles (*39*) or cadavers (*40*). Histologic bone marrow and tumor samples would provide additional insight beyond this study, such as the maximum tumor size that could be treated with ^{223}Ra. However, in terms of comparing the relative merits of these radionuclides, we would expect results similar to those obtained in this report.

CONCLUSION

^{223}Ra may provide both a more effective radiation source and a safer radiation source for red marrow than does ^{89}Sr. Dose estimates in this study supplied additional justification for ^{223}Ra as a novel approach to treating micrometastatic cancer deposited on the surfaces of the skeleton. Compared with the current suite of β-emitters used in palliation of bone pain, ^{223}Ra localized at bone surfaces (and perhaps taken up by calcified, osteogenic tumors) can, together with its daughter radionuclides, deliver an intense and highly local radiation dose of α-particles with bone marrow sparing. Further studies—for example, on an appropriate skeletal metastasis model—are therefore warranted.

ACKNOWLEDGMENTS

The authors thank Solveig Garmann Vik and Marita Martinsen at the Norwegian Radium Hospital for their skillful assistance with the animal experiments.

REFERENCES

1. Silberstein EB. The treatment of painful osseous metastases with phosphorous-32 labeled phosphates. *Semin Oncol.* 1993;20:10–21.
2. Ackery D, Yardley J. Radionuclide-targeted therapy for the management of metastatic bone pain. *Semin Oncol.* 1993;20(suppl 2):27–31.
3. Silberstein EB. Dosage and response in radiopharmaceutical therapy of painful osseous metastases. *J Nucl Med.* 1996;37:249–252.
4. Bouchet LG, Bolch WE, Goddu SM, Howell RW, Rao DV. Considerations in the selection of radiopharmaceuticals for palliation of bone pain from metastatic osseous lesions. *J Nucl Med.* 2000;41:682–687.
5. Goddu SM, Bishayee A, Bouchet LG, Bolch WE, Rao DV, Howell R. Marrow toxicity of ^{33}P- versus ^{32}P-orthophosphate: implications for therapy of bone pain and bone metastases. *J Nucl Med.* 2000;41:941–951.
6. Krishnamurthy GT, Krishnamurthy S. Radionuclides for metastatic bone pain palliation: a need for rational re-evaluation in the new millennium. *J Nucl Med.* 2000;41:688–691.
7. Serafini AN, Houston SJ, Resche I, et al. Palliation of pain associated with metastatic bone cancer using samarium-153 lexidronam: a double-blind placebo-controlled clinical trial. *J Clin Oncol.* 1998;16:1574–1581.
8. Maxon HR, Schroder LE, Hertzberg VS, et al. Rhenium-186(Sn)HEDP for treatment of painful osseous metastases: results of a double-blind crossover comparison with placebo. *J Nucl Med.* 1991;32:1877–1881.
9. Atkins H-L, Mausner LF, Srivastava SC, Meinken GE, Cabahug GE, D'Alessandro T. Tin-117m(4+)DTPA for palliation of pain from osseous metastases: a pilot study. *J Nucl Med.* 1995;36:725–729.
10. Feinendegen LE, McClure JJ. α-emitters for medical therapy. *Radiat Res.* 1997; 148:195–201.
11. Ritter MA, Cleaver JE, Tobias CA. High-LET radiations induce a large proportion of non-rejoining DNA breaks. *Nature.* 1977;266:653–655.
12. Larsen RH, Murud KM, Akabani G, Hoff P, Bruland ØS, Zalutsky MR. ^{211}At- and ^{131}I-labeled bisphosphonates with high in vivo stability and bone accumulation. *J Nucl Med.* 1999;40:1197–1203.
13. Hassfjell SP, Hoff P, Bruland ØS, Alstad J. ^{212}Pb/^{212}Bi-EDTMP: synthesis and biodistribution of a novel bone seeking alpha-emitting radiopharmaceutical. *J Labelled Compds Radiopharm.* 1994;34:717–734.
14. Hassfjell SP, Bruland ØS, Hoff P. ^{212}Bi-DOTMP: an alpha particle emitting bone seeking agent for targeted radiotherapy. *Nucl Med Biol.* 1997;24:231–237.
15. Howell RW, Goddu SM, Narra VR, Fisher DR, Schenter RE, Rao DV. Radiotoxicity of gadolinium-148 and radium-223 in mouse testes: relative biological effectiveness of alpha-particle emitters *in vivo. Radiat Res.* 1997;147:342–348.
16. Tiepolt C, Gruning T, Franke WG. Renaissance of ^{224}Ra treatment in ankylosing spondylitis [abstract]. *J Nucl Med.* 2001;42(suppl):128P.
17. Delikan O. Preparation of ^{224}Ra for therapy of ankylosing spondylitis. *Health Phys.* 1978;35:21–24.
18. Nekolla EA, Kellerer AM, Kuse-Isingschulte M, Eder E, Spiess H. Malignancies in patients treated with high doses of radium-224. *Radiat Res.* 1999;152:S3–S7.
19. Nekolla EA, Kreisheimer M, Kellerer AM, Kuse-Isingschulte M, Gössner W, Spiess H. Induction of malignant bone tumors in radium-224 patients: risk estimates based on the improved dosimetry. *Radiat Res.* 2000;153:93–103.
20. Lloyd RD, Mays CW, Taylor GN, Atherton DR, Bruenger FW, Jones CW. Radium-224 retention, distribution, and dosimetry in beagles. *Radiat Res.* 1982; 92:280–295.
21. Müller WA. Studies on short-lived internal α-emitters in mice and rats. I. ^{224}Ra. *Int J Radiat Biol.* 1971;20:27–38.
22. Henriksen G, Alstad J, Hoff P, Larsen RH. ^{223}Ra for endo-radiotherapeutic applications prepared from an immobilized ^{227}Ac/^{227}Th source. *Radiochim Acta.* 2001;89:661–666.
23. Ekstrøm L, Spanier R. *The ENSDF Radioactivity Data Base for IBM-PC and Computer Network Access.* Lund, Sweden: Department of Physics, University of Lund; 1989.
24. *Guidelines on the Care of Laboratory Animals and Their Use for Scientific Purposes.* London, U.K.: Royal Society/Universities Federation for Animal Welfare; 1987.
25. Roeske JC, Chen GTY, Atcher RW, et al. Modeling of dose to tumor and normal tissue from intraperitoneal radioimmunotherapy with alpha and beta emitters. *Int J Radiat Oncol Biol Phys.* 1990;19:1539–1548.
26. International Commission on Radiation Units and Measurements (ICRU 49). *Stopping Powers and Ranges for Protons and Alpha Particles.* Bethesda, MD: International Commission on Radiation Units and Measurements; 1993.
27. International Commission on Radiological Protection (ICRP 70). *Basic Anatomical and Physiological Data for Use in Radiological Protection: The Skeleton.* Oxford, U.K.: Elsevier Science Ltd.; 1995.
28. Fisher DR, Sgouros G. Dosimetry of radium-223 and progeny. In: Schlafke-Stelson AT, Watson EE, eds. *Proceedings of the Sixth International Radiopharmaceutical Dosimetry Symposium.* Oak Ridge, TN: Oak Ridge Institute for Science and Education; 1999:375–391. ORISE 99-0164.
29. Fisher DR. Internal dosimetry for systemic radiation therapy. *Semin Rad Oncol.* 2000;10:123–132.
30. Loevinger R, Budinger TF, Watson EE. *MIRD Primer for Absorbed Dose Calculations.* Revised ed. New York, NY: Society of Nuclear Medicine; 1991.
31. Berger MJ. Distributions of absorbed dose around point sources of electrons and beta particles in water and other media: MIRD pamphlet no. 7. *J Nucl Med.* 1971;12(suppl 5):5–23.
32. Hui TE, Fisher DR, Press OW, Weinstein JN, Badger CC, Bernstein ID. Localized beta dosimetry of I-131-labeled antibodies in follicular lymphoma. *Med Phys.* 1992;19:97–104.
33. Olko P, Booz J. Energy deposition by protons and alpha particles in spherical sites of nanometer to micrometer diameter. *Radiat Environ Biophys.* 1990;28:1–17.
34. Hall EJ. *Radiology for the Radiologist.* 4th ed. Philadelphia, PA: JB Lippincott Co.; 1994:153–164.
35. Yoneda T, Sasaki A, Dunstan C, et al. Inhibition of osteolytic bone metastases of breast cancer by combined treatment with the bisphosphonate ibandronate and tissue inhibitor of the matrix metalloproteinase-2. *J Clin Invest.* 1997;99:2509–2517.
36. Rosen LS, Gordon D, Kaminski M, et al. Zoledronic acid versus pamidronate in the treatment of skeletal metastases in patients with breast cancer or osteolytic lesions of multiple myeloma: a phase III, double-blind, comparative trial. *Cancer J.* 2001;7:377–387.
37. Coleman RE. Metastatic bone disease: clinical features, pathophysiology and treatment strategies. *Cancer Treat Rev.* 2001;27:165–176.
38. Henriksen G, Breistøl K, Bruland ØS, et al. Significant antitumor effect from bone-seeking, α-particle emitting ^{223}Ra demonstrated in an experimental skeletal metastases model. *Cancer Res.* 2002;62:3120–3125.
39. Akabani G, Zalutsky MR. Microdosimetry of astatine-211 using histological images: application to bone marrow. *Radiat Res.* 1997;148:599–607.
40. Charlton DE, Salmon PL, Utteridge TD. Monte Carlo/numerical treatment of alpha-particle spectra from sources buried in bone and resultant doses to surface cells. *Int J Radiat Biol.* 1998;73:89–92.